

## Effects of transmission factors and matrix elements on angular distribution of photoemission from Ag(111)

D. J. Spanjaard,\* D. W. Jepsen, and P. M. Marcus

IBM Thomas J. Watson Research Center, Yorktown Heights, New York 10598

(Received 17 February 1976)

The theory of the angularly dependent photoemission from a semi-infinite crystal as a one-step process is briefly reviewed, starting from the formulas of Adawi and using surface-matched wave functions in both upper and lower states and absorption in the upper state. We derive conditions under which the three-step model can be justified. The angle-resolved photoemission from Ag(111) is calculated from the three-step formula with transmission factors and matrix elements obtained from a self-consistent potential for Ag, and compared with experimental data of Gustafsson *et al.* The transmission factor has a small effect, amounting to a nearly constant factor of 0.55 at all angles over the energies of interest; the dependence on the angle of incidence of the radiation is much stronger and is in agreement with observation.

### I. INTRODUCTION

In the last few years there has been a growing interest in the study of the directional dependence of ultraviolet photoemission from single-crystal surfaces. It has been shown that the emission depends on the polarization of the light,<sup>1-4</sup> that it varies with the polar<sup>3-6</sup> and azimuthal<sup>1,2</sup> angles of observation, and that the emission can be different from different faces of the same crystal.<sup>7,8</sup> In the most recent work it has been possible to map out the electron intensity as a function of angle in some detail.<sup>9-13</sup>

These asymmetries arise from the variation in the electronic states involved in the phototransition as the geometry of the experiment is changed. In principle one could hope to examine the bands of the crystal throughout the Brillouin zone<sup>14,15</sup> in the same manner as the phonon dispersion is mapped in inelastic-neutron-scattering experiments. The electronic case is clearly more difficult because there is both a lower and an upper electronic state which are probed rather than the single phonon in the neutron experiment. Furthermore, the matrix element which describes the interaction of light with an electronic system is more complicated than the simple pseudopotential interaction of the phonon with the neutron.

Contributions from surface states also occur in the observed spectra,<sup>16,17</sup> on the one hand making interpretation of the experiment more complicated, and on the other hand increasing the variety of information which can be obtained. At the energies at which the emitted electrons are collected, only those electrons from a few outer layers of the crystal are likely to reach the vacuum outside the surface without losing a very large part of their energy by plasmon or electron-hole pair excitation. Thus the surface states of the crystal, which

are normally localized in these layers, are found to contribute to a degree comparable to the bulk states. It is not yet clear how the altered environment in this narrow region (it can be as small as three atom layers) near the surface can modify the contribution which arises from the bulk states of the crystal. Some of the experimentally observed structure presently attributed to surface states may in fact arise in this way. The work reported here was undertaken to elucidate some of the effects noted above, particularly the transmission of the electrons from the periodic potential of the crystal into vacuum.

We have chosen the (111) face of silver for study because the angular photoemission has been measured.<sup>3,6</sup> The total photoemission as a function of crystal face and photon energy<sup>9</sup> has also been measured for silver. At the low photon energy of 7.8 eV, studied here because the angle-dependent measurements were made at that energy, only *s* and *p* bands need be considered in the description of the data. In fact, many of the results can be explained quite successfully by a simple nearly-free-electron model using only two bands. The simple model is not able to explain all features of the data, particularly the existence of photoemission for light incident normal to the surface, and the work reported here gives this intensity properly. Our results give a better fit to the experimental data than the previous work of Schaich,<sup>18</sup> probably because we have used a self-consistent potential and an accurate band-structure procedure rather than a pseudopotential approach for silver. We use a Korringa-Kohn-Rostoker-type band method and matrix elements formed from the resulting wave functions to describe the transition. The photoemission is calculated as a function of angle by formulas like the usual three-step model,<sup>19</sup> which are obtained in a natural way from the

single-step formulation of the problem due to Adawi<sup>20</sup> and Mahan,<sup>21</sup> with no error in the reduction when the conditions derived for the direct transition model are satisfied. The calculation we give of the transmission coefficient through the surface, which comprises the third step, has not been done previously using an accurate potential, and is therefore of particular interest. Assuming specular matching in the surface, we obtain a transmission coefficient which is essentially constant in energy and has a value of about 0.55 under those conditions where transmission is permitted by the simple step barrier model.

The experimental data of Gustafsson, Nilsson and Wallden<sup>3</sup> contain a 40% component that does not show the angular variation which follows from the direct-transition condition resulting from our theory. This component must arise from some type of surface photoemission. It cannot arise from scattering of bulk electrons in the neighborhood of the surface because it is found to persist even when there are no bulk electrons.<sup>22</sup> Feurbacher and Fitton<sup>7</sup> also found that such emission associated with the surface is necessary to explain much of their data on tungsten. The explanation of the data of Nilsson and Eastman<sup>8</sup> probably also requires the further assumption that there was additional scattering in the surface of their samples.

## II. REDUCTION OF THE ONE-STEP FORMULA TO THE THREE-STEP MODEL

Adawi has derived a formal expression for the photoemission from the surface of a crystalline solid using a general formulation of scattering theory.<sup>20</sup> He finds that the current density proportional to the light intensity, at a final energy  $E^f = E^i + \hbar\omega$ , in a solid angle  $d\Omega$  is given in Gaussian units by<sup>23</sup>

$$dI_\nu = -(emk_f/4\hbar^3\pi^2) d\Omega |M_\nu|^2, \quad (1)$$

with

$$M_\nu = (\Psi^{L*} | H^i | \phi_\nu^i),$$

$$H^i = (-ie\hbar/m\omega) \vec{\mathcal{E}}(\vec{r}) \cdot \vec{\nabla},$$

$$\vec{\mathcal{E}}(\vec{r}, t) = 2 \operatorname{Re}[\vec{\mathcal{E}}(\vec{r})e^{-i\omega t}],$$

where  $k_f$  is the wave vector of the outgoing electron,  $\vec{\mathcal{E}}(\vec{r})$  is the electric field vector,  $\omega$  the angular frequency of the light wave,  $\hbar$  is Planck's constant over  $2\pi$ ,  $c$  is the velocity of light, and  $e$  and  $m$  are the charge and mass of the electron, respectively. The matrix element  $M_\nu$  contains the  $\nu$ th initial wave function  $\phi_\nu^i$  at an energy  $E^i$  below the Fermi level, and  $\Psi^{L*}$  the complex conjugate of a wave function which would describe the low-energy electron diffraction of an electron coming

from the direction of the photoemission detector at the energy  $E^i + \hbar\omega$ . The final wave  $\Psi^{L*}$  is normalized to one electron per unit volume in the outgoing wave in vacuum, i.e., the outwave is a plane wave of unit amplitude, and the initial wave  $\phi_\nu^i$  is normalized to the volume of the crystal  $V$ . We have changed the arrangement of numerical factors slightly from Adawi's paper. Adawi actually assumed a model in which the crystal potential depends only on the distance into the crystal, but his formalism remains unchanged when this assumption is dropped.

The wave functions in this formula all have the same reduced wave vector in the plane of the surface  $k_{\parallel} = (k_x, k_y)$ , which is determined by the angle of observation. An initial state  $\phi^i$  in photoemission is a wave function consisting of a propagating Bloch wave moving toward the surface plus the reflected Bloch waves, propagating and evanescent, necessary to match this incident wave to evanescent plane waves in vacuum decreasing away from the surface. There may be a number of such initial states which give contributions to the photoemission. We do not include possible surface states as initial states in this work, although this could be done.

The formulation of Adawi describes the photoemission from a single initial state. For the photoemission considered here, there are many such initial states which are extended over the whole crystal. As we shall see, only the part of each wave function near the surface actually contributes to the emission. The proper normalization of this initial state can be obtained by requiring that a standing initial-state Bloch wave between the front and back surfaces of the crystal be normalized to the crystal volume. The density of states is then obtained by counting these same states.<sup>24</sup> It is clearly possible to restrict the integration in the matrix element to the volume in a cylinder under a single unit mesh of the surface, provided we multiply the resulting matrix element by the number of meshes in the surface of the crystal. If we change the normalization of the initial wave functions to this same volume, we must multiply the resulting matrix element by the reciprocal square root of the same factor so that this factor occurs in the final full expression to the first power. We need only consider initial waves with components  $k_x, k_y$ , of reduced  $k$  in the plane of the surface which match up with the corresponding  $k$  components of the final state, but there will be a large number of states closely spaced in their values of  $k_x$  perpendicular to the surface which fall within the range  $E, E + dE$  of initial energies. The number of states with  $k_x$  falling within the required range is  $2D dE / (\pi dE_\nu / dk_x)$ , where  $D$  is the

thickness of the crystal, and  $E_\nu$  is the band energy of the  $\nu$ th incident Bloch wave. Here a factor of 2 arises from summing spin states. By making the further change of the normalization of the initial states to a unit cell of the bulk rather than a cylinder through the crystal under a surface mesh, we can eliminate the factor  $D$  occurring in this formula in favor of a factor of " $a$ ," the thickness of a unit cell measured perpendicular to the surface. Hence it is convenient to introduce a new initial wave function normalized to 1 over an "average" unit cell, which is related to  $\phi_\nu^i$  by

$$\Psi_\nu^i = (V/Aa)^{1/2} \phi_\nu^i,$$

where again  $V$  is the volume of the crystal, and  $Aa$  is the volume of a unit cell. These changes give

$$d^2I = -\frac{e^3 k_y a S d\Omega dE}{2\pi^3 \hbar^2 m \omega^2 A} \sum_\nu \frac{1}{v_\nu} \left| \int_{AD} \Psi^L \vec{\mathcal{E}}(z) \cdot \vec{\nabla} \Psi_\nu^i d^3r \right|^2, \quad (2)$$

where

$$v_\nu = \frac{1}{\hbar} \frac{\partial E_\nu}{\partial \mathbf{k}_z},$$

and the integration is over a column of area  $A$ , depth  $D$ . Here  $S$  is the area of the surface,  $A$  is the area of a unit mesh in this surface, and the  $\nu$  summation is over initial states with incident Bloch waves with group velocities  $v_\nu$ .

Following Mahan,<sup>21</sup> we can transform this formula to an expression representing the usual three-step model of photoemission when the electron mean free path in the upper state is sufficiently long. We shall review this transformation here because we wish to examine the conditions under which it is valid. A more complete treatment of the theory of photoemission has been given by Feibelman and Eastman.<sup>25</sup>

We split up the integration in the matrix element into the sum of an integral over the surface region of the crystal and an integral over the column of undisturbed bulk cells underneath. The integration over the surface region will include a contribution from the region of the potential step between crystal and vacuum, from any adsorption layers, and from any greatly disturbed layers of substrate atoms. The integral over the bulk region underneath can be split into integrals over an infinite number of cells of identical structure. In the bulk of the crystal both the lower and upper wave functions of the transition,  $\Psi^i$  and  $\Psi^L$  can be represented in terms of propagating and evanescent Bloch waves in the form

$$\begin{aligned} \Psi^L &= \sum_n \beta_n^+ b_n(\vec{\mathbf{r}}, -\vec{\mathbf{k}}_\parallel, E^f), \\ \Psi_\nu^i &= \sum_m \beta_{\nu m}^i b_m(\vec{\mathbf{r}}, \vec{\mathbf{k}}_\parallel, E^i). \end{aligned} \quad (3)$$

The summation in the expression for  $\Psi^L$ , the complex conjugate of the final state, includes only Bloch waves carrying flux into the crystal as in the low-energy-electron-diffraction (LEED) experiment, but the expression for the initial state contains waves carrying flux both toward and away from the surface. Note that when  $k_x$ ,  $k_y$ , and the energy  $E$  of a Bloch wave in a given band are known,  $k_z$  is determined, but there may be different states from different bands at this energy with the same  $k_x$  and  $k_y$  but differing  $k_z$  values. We label these different propagating waves, along with the evanescent waves which occur for the same  $k_x$ ,  $k_y$  and energy, by the  $m$  and  $n$  indices, and include them all in the sums. Complex  $k_z$ 's arise for evanescent waves and will occur more generally when inelastic scattering effects are included below. Each propagating or evanescent Bloch wave satisfies the relation

$$\begin{aligned} b_i(x + a_{3x}, y + a_{3y}, z + a_{3z}, \vec{\mathbf{k}}_\parallel, E) \\ = \exp[i(\mathbf{k}_x a_{3x} + k_y a_{3y} + k_z a)] b_i(\vec{\mathbf{r}}, \vec{\mathbf{k}}_\parallel, E), \end{aligned} \quad (4)$$

where  $\vec{\mathbf{a}}_3$  is a lattice vector into the crystal forming a primitive set with two lattice vectors in the plane of the surface, and  $a_{3z} = a$ , the cell thickness used in (2).

In finding the wave functions in the solid, particularly that of the upper state, we consider a Schrödinger equation which includes an imaginary contribution to the potential and find solutions for real  $k_x$ ,  $k_y$ , and  $E$  but complex  $k_z$ , as has been done in low energy electron diffraction studies.<sup>26-29</sup> It can be verified that the formalism of Adawi is still valid when this is done. When this imaginary term is present, the difference between a propagating Bloch wave and an evanescent Bloch wave is not sharp, but the  $k_z$  value of a propagating wave is nearly real with a small imaginary part resulting from inelastic scattering, whereas an evanescent wave has an imaginary part both from inelastic scattering and from a band gap which localizes it more strongly to the neighborhood of the surface. The amplitude of the light wave has the  $z$  dependence

$$\vec{\mathcal{E}}(\vec{\mathbf{r}}) = \vec{\mathcal{E}}_0 e^{-\alpha_0 z/2}, \quad (5)$$

where  $\alpha_0$  is the absorption constant (of the intensity). We have assumed here that the light has a long wavelength compared to the electron wavelengths.

Using (3)–(5) in (2), the contributions of the cells in the successive layers of the bulk below the surface form the terms of a geometrical ser-

ies, which may be summed to give

$$d^2I = -\frac{e^3 k_f a S d \Omega dE}{2\pi^3 \hbar^2 m \omega^2 A} \times \sum_v \frac{1}{v_v} \left| M_v^s + \sum_{mn} \beta_{vm}^i \beta_{n}^f \Delta_{mn} e^{-\alpha_0 d/2} M_{mn}^B \right|^2, \\ M_v^s = \int_{SL} \Psi^L(\vec{r}) e^{-\alpha_0 z/2} \vec{\mathcal{E}}_0 \cdot \vec{\nabla} \Psi_v^i(\vec{r}) d^3r, \quad (6) \\ M_{mn}^B = \int_0^a e^{-\alpha_0 z/2} dz \int_A b_m(\vec{r}) \vec{\mathcal{E}}_0 \cdot \vec{\nabla} b_n(\vec{r}) dx dy, \\ \Delta_{mn} = \left\{ 1 - \exp[i(k_m^i + k_n^f + \frac{1}{2} i \alpha_0) a] \right\}^{-1}.$$

Here the second integral is taken over a typical cell in the bulk, assumed to begin a distance  $d$  down from the surface, and first integration is over SL, the volume under a unit mesh of the surface containing the surface layer down to a distance  $d$ .

Under conditions where the escape depth is not too short, coherence of the waves excited from different layers requires that the reduced  $k_z$  of the initial and final Bloch waves involved in the photon-induced transition be at least approximately opposite. This is really the condition that the  $k_z$  of the final state, understood to be the complex conjugate of the LEED wave function, be nearly equal to that of the initial state, i.e., the usual  $k_z$  conservation in the three-step model of photoemission. Such a condition is usually satisfied by at most one pair of waves in the double sum in Eq. (6). As discussed by Mahan, the absolute square of a typical term of the double sum contains the factor  $|\Delta_{mn}|^2$  of the form

$$|\Delta_{mn}|^2 = [1 - \exp(-a/l) + 4 \exp(-a/l) \sin^2(\Delta ka/2)]^{-1}, \quad (7)$$

where

$$1/l = \text{Im}(k_{zm}^i + k_{zn}^f) + \frac{1}{2} \alpha_0, \quad \Delta k = \text{Re}(k_{zm}^i + k_{zn}^f).$$

Note that the imaginary parts of both  $k$ 's give a positive contribution to  $l$ . The expression in Eq. (7) is plotted in Fig. 1 for several values of  $a/l$ , where we see that this function approaches a  $\delta$  function in  $\Delta k$ , and thus that  $k_z$  is conserved, if  $l$  is greater than about four layers. For transitions between propagating Bloch states the principal contribution to  $l$  comes from the mean free path of the electron in the upper state, and since  $l$  measures the decay of an amplitude, it is given closely by  $\frac{1}{2}$  the value of the mean free path in the upper state. The total area under each of the curves shown in Fig. 1 is  $2\pi/[1 - \exp(-2a/l)]$ , so that the total photoemission increases with  $l$  and becomes proportional to  $\pi l/a$  for large  $l$ , as given by

Mahan. In silver the value of  $l$  varies considerably with energy according to simple estimates,<sup>30</sup> but is always greater than five layers, so that  $k_z$  conservation in transitions between Bloch states must always be closely satisfied. Since different Bloch waves have different  $k_z$  values, we may assume that at most one pair of initial and final Bloch states contributes to the bulk part of the photoemission in Eq. (6). In fact one can expect to find  $k_z$  conserved, and hence a nonzero term only along a curve in theta, phi solid-angle space. The spread of the curve in Fig. 1 should be observable experimentally as a spread in angle about these curves in angle space given by the direct transition model. Since the detector in the experiments considered here collects all waves for which the final  $k_z$  is nearly equal to the initial  $k_z$ , we may use the integrated area multiplied by the  $\delta$  function  $\delta(\Delta ka)$  for the expression in Eq. (7) as suggested by Mahan,

$$|\Delta_{mn}|^2 \cong \frac{2\pi}{1 - \exp(-2a/l)} \delta(\Delta ka). \quad (8)$$

To obtain formulas nearer to those usually given for the three-step model, this  $\delta$  function can be replaced by  $v_f \delta(E^i + \hbar\omega - E^f)$ , where  $v_f = \partial E^f / \partial k_z$  is the group velocity of the final Bloch wave directed toward the surface. Furthermore, since the integrated area for the usual propagating waves having large  $l$ 's will be much larger than the area for evanescent waves at the surface which decay rapidly into the crystal, we shall also neglect any contributions to the photoemission from evanes-

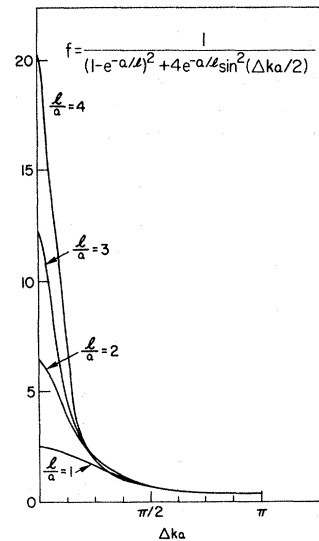


FIG. 1. Magnitude of the photoemission as a function of  $\Delta ka$ , the deviation from  $k_z$  conservation, for various values of the mean free path  $l$ .

cent waves. Note that the factor  $2\pi/[1 - \exp(-2a/l)]$  contains and describes the probability that the electron reach the surface from the point of emission. No further analysis or approximation is required to take this process, the second step of the usual three-step model, into account.

For a surface that preserves its bulk structure up to the vacuum,  $d$  is nearly equal to zero and the first term in Eq. (6) will contain only the photoemission from the potential step from vacuum to crystal discussed by Mitchell<sup>31</sup> and Makinson.<sup>32</sup> The square of this term should give a contribution with a broad slowly varying distribution over angle, and we shall not consider it further. The interference between the surface and bulk terms should modify the observed angle dependence, but we will not calculate this effect here. For light normal to the surface the first term and hence also this interference effect disappears.

Hence we are left with only the contribution from at most a single pair of initial and final states in the second term conserving all components of  $\vec{k}$ . It is shown in the Appendix that when we sum over all possible initial states  $\nu$  the factor  $|\beta_{\nu m}^i|^2/v_\nu$  gives the factor  $1/v_m$  for any Bloch wave  $m$  which is normalized to unit volume.<sup>25</sup> Hence we shall make this substitution. This gives

$$d^2I = \frac{-e^3 k_f a S d\Omega dE |\beta_n^f|^2 v_f \delta(E^f - E^i - \hbar\omega)}{\pi^2 \hbar^2 m \omega^2 v_m [1 - \exp(-2a/l)]} |M_{mn}^B|^2. \quad (9)$$

The factor  $|\beta_n^f|^2 v_f$  is the flux produced in a LEED experiment in the time-reversed form of the  $n$ th Bloch state. Since the incident LEED wave was assumed to have a standard flux incident on the surface, this quantity is closely related to the transmission coefficient through the surface, and describes the third step in the usual three-step model of photoemission. Thus the usual expressions for the three-step model can be reduced to the expression of Eq. (9). Actually, for angular photoemission measurements the  $\delta$  function in  $\Delta k$  contained in Eq. (8) is more appropriate than the  $\delta$  function in energy replacing it here, because the deviations from delta function behavior can manifest themselves in angular spreads which are more easily interpreted in terms of a spread in  $\Delta k$ .

### III. METHOD OF CALCULATION

The calculational procedures used in this work are an adaptation of the methods, and in fact the computer programs of Janak, Williams, and Morruzzi<sup>33</sup> for calculating angle and surface-averaged bulk photoemission, to a single-crystal face with the inclusion of an accurate calculation of the

transmission coefficient from the crystalline medium to vacuum. For the (111) face of an fcc structure like the silver lattice, six reduced zones each  $\frac{1}{48}$ th of the full Brillouin zone were considered, since the symmetry of the crystal is lowered by introducing the surface plane. Following Janak, Williams, and Morruzzi, each reduced zone was divided into 10 100 small cubes, and for each possible energy of the escaping electron, line segments were found within some of the cubes along which momentum and energy conservation were properly satisfied to lowest order in the cell size. The lengths of these line segments were multiplied by the matrix elements and transmission factors to a given detector and the result summed over the contributing cubes. Generally the transmission into several detectors subtending different solid angle sectors around the sample can be summed in the same calculation. Since unpolarized light has been used in the experiments, the square of the matrix element was averaged over  $E$  field directions in a plane perpendicular to the incident direction of the light. The effects of inelastic scattering of the electrons were neglected in the calculation of all quantities other than the damping factor  $l$ .

The calculation of the transmission coefficient through the surface requires new procedures which were adapted from the methods and computer programs used in LEED calculations.<sup>34</sup> In the formalism used in the LEED work, the amplitudes  $\beta_1^+, \beta_2^+, \beta_3^+, \dots$  of Bloch waves moving into the crystal from the surface and the amplitudes  $\beta_1^-, \beta_2^-, \beta_3^-, \dots$  of Bloch waves moving from inside the crystal toward the surface can be related to the amplitudes  $\alpha_1^+, \alpha_2^+, \alpha_3^+, \dots$  and  $\alpha_1^-, \alpha_2^-, \alpha_3^-, \dots$  of the matching plane waves in vacuum by matrix equations of the form<sup>34</sup>

$$G(\alpha_1^+ \dots \alpha_1^- \dots)^T = (\beta_1^+ \dots \beta_1^- \dots)^T \quad (10)$$

(where superscript  $T$  for transpose indicates the column vector), and  $G$  is a matrix depending on the crystal. In this work, unlike the LEED work, we choose one Bloch wave moving toward the surface to have nonzero amplitude and require that there be no plane waves in vacuum moving toward the surface. Equation (10) then reduces to a set of linear equations for the amplitudes of the plane waves leaving the surface in vacuum. The flux in each of these waves can be calculated and hence the transmission of a Bloch wave of unit flux through the surface to plane waves into any solid angle outside the crystal.

The procedure just described is slightly different from the prescription specified by the one-step model of photoemission. However, if only

one Bloch wave in the upper state takes part in the emission process we may apply the principle of reciprocity.<sup>35</sup> The transmission through the surface found above is shown by reciprocity to be the same as for a source of electrons outside the crystal at the position of collection in the experiment and a detector inside the crystal sensitive to this Bloch wave. These latter conditions describe the transmission coefficient given by the LEED wave function. However, the calculation of the transmission out of the crystal is slightly shorter.

#### IV. RESULTS OF THE CALCULATION

Calculations were performed for the (111) face of a silver crystal using the wave functions obtained from the self-consistent Hartree-Fock-Slater potential of Snow<sup>36</sup> with the exchange-correlation coefficient  $\alpha = \frac{5}{6}$ . The intensity of the light in the crystal and its rate of absorption were obtained from the measured optical constants<sup>37</sup> in the obvious way. The mean free path of the excited electrons was estimated from the data of Kanter,<sup>38</sup> and fitted to the random  $k$  model of Kane<sup>39</sup> as described by Janak *et al.*<sup>33</sup> The result obtained for the lifetime in rydberg units was  $t = 150(\Delta E)^{-3.6}$ , where  $\Delta E$  is the energy above the muffin tin zero in rydbergs. A continuous hyperbolic-tangent step about  $\frac{1}{1000}$  a.u. wide was used as the interface between crystal and vacuum in the calculation of the transmission factor. This was chosen to approximate the sharp step used by us in similar calculations on surface states.<sup>40</sup> In our model the crystal is oriented so that an atom of the top layer lies at the origin with neighboring atoms of the top layer on the  $x$  and  $y$  axes taken at an angle of 60 deg. An atom of the layer beneath the top layer was located at  $(\frac{1}{3}, \frac{1}{3})$  in units of the surface mesh.

The calculation was set up to model an experiment in which the detectors were arranged in the following way: The range of polar angle from normal incidence to grazing was divided into nine sectors, each with the same solid angle. The angles delimiting the sectors thus came out to be 0.0, 27.27, 38.94, 48.19, 56.25, 63.61, 70.53, 77.16, 83.62, and 90.00 deg. The range of azimuthal angle was divided into 15-deg sectors. A detector measured all electrons emitted within each combination of  $\theta$  and  $\varphi$  ranges.

In Fig. 2 we show the energy distribution of electrons entering each of the counters spanning the range of polar angle from 27.27 to 38.94 deg. We note a small but relatively rapid variation of the number of electrons emitted into the various azimuthal sectors as a function of energy. This rapid variation is probably produced by the reflection of the electron back to the emitting atom from neigh-

boring atoms and the resulting effect on the emission process. A similar but more pronounced rapid variation has been seen experimentally in the photoemission from semiconductors.<sup>10</sup>

In Fig. 3 we show the number of electrons entering each sector in the range of polar angles with all azimuthal angles included. It is useful to compare these results with the experimental data of Gustafsson, Nilsson, and Wallden,<sup>3</sup> who used a similar arrangement of counters. Comparing our results with the dashed curve 1, we notice that both in the theory and the experiment the electrons from the states of lowest energy come out of the surface nearer to the normal, e.g., the electrons below 1.0 eV are almost all in  $\Delta\theta_1$ , whereas dashed curve 2 corresponds to  $\Delta\theta_2$ . This effect has already been explained in terms of a simple two-band nearly-free-electron model,<sup>6,8</sup> and follows from the general shape of the bands involved in the transition, and the requirement of  $k$  conservation. The emission at large angles is markedly smaller than at lower angles because this emission at large angles arises from plane-wave components of the Bloch state which are zero in the limit of free-electron bands as shown in  $\Delta\theta_5$  and dashed curve 3. Such emission corresponds to the secondary cones in the treatment of Mahan.

In Fig. 4 we show the energy dependence of the total photocurrent for photons incident at three

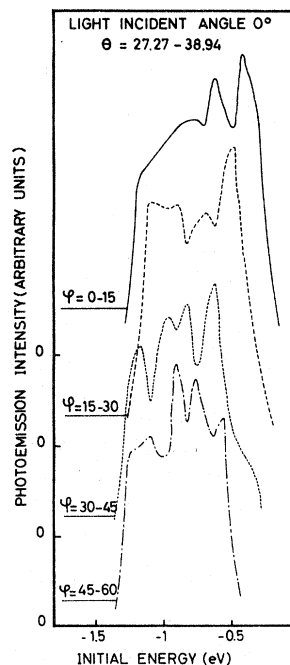


FIG. 2. Calculated variation of the photoemission intensity as a function of energy for various ranges of azimuthal angle with the polar angle in the range  $27.27 \leq \theta \leq 38.96$  deg.

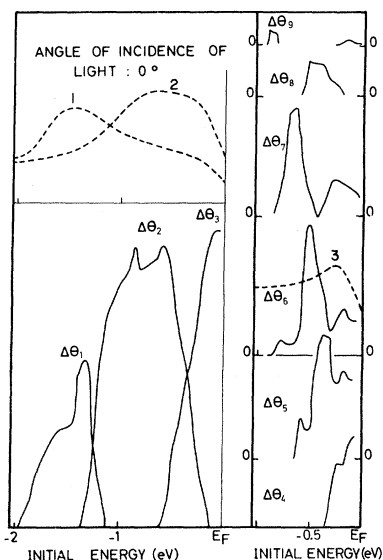


FIG. 3. Variation of the photoemission intensity as a function of energy for the following ranges (of equal solid angle) of the polar angle in degrees:  $\Delta\theta_1=0.00-27.27$ ,  $\Delta\theta_2=27.27-38.94$ ,  $\Delta\theta_3=38.94-48.19$ ,  $\Delta\theta_4=48.19-56.25$ ,  $\Delta\theta_5=56.25-63.61$ ,  $\Delta\theta_6=63.61-70.53$ ,  $\Delta\theta_7=70.53-77.16$ ,  $\Delta\theta_8=77.16-83.62$ ,  $\Delta\theta_9=83.62-90.00$ . Emission for all azimuthal angles is included in each range. The dashed curves marked 1, 2, 3 are the experimental curves of Refs. 4 and 5 covering ranges in  $\theta$ -1:11-26, 2:3-48, 3:53-68.

different angles: normal incidence, the  $[110]$  direction, and the  $[1\bar{1}\bar{1}]$  direction. The change seen in the spectrum arises from the dependence of the matrix element  $M_{mn}^B$  in Eq. (9) on the polarization of the photons. If the wave functions in this matrix element are approximated by the plane waves appropriate to a simple nearly-free-electron, two-band model of the energy states involved in this transition, we find that, since the upper and lower states differ by a reciprocal-lattice vector perpendicular to the surface, the transition dipole is in this direction. Thus in this crude approximation the emission should be proportional to the square of the sine of the angle of the photon beam from the normal to the surface. In particular, the emission should disappear when the photons are incident normal to the surface. Our calculations with better wave functions give emission at normal incidence, but show a reduced intensity as one moves toward the normal, particularly at the lower energies, where the emission arises from transitions between nearly parabolic bands. At the lowest energies the emission arises from transitions near  $k=0$ , where the momentum matrix element must be perpendicular to the surface by symmetry. This gives the shape of the drop to zero intensity

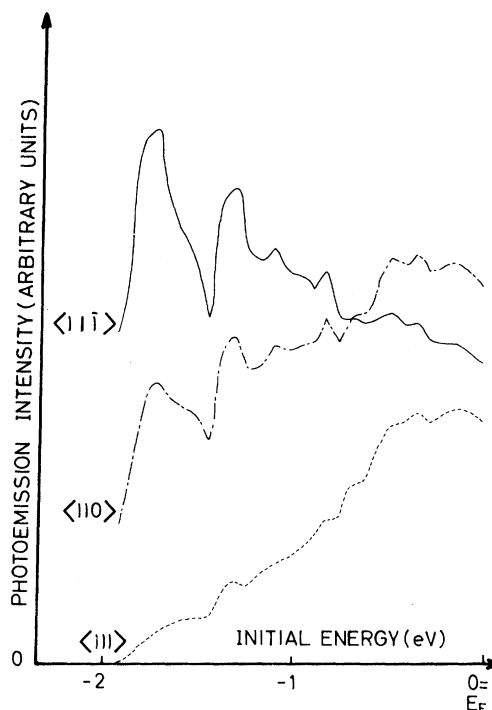


FIG. 4. Total photoemission intensity as a function of energy for three directions of incidence of the light.

seen at this end of the spectrum. The experimental results<sup>4</sup> show a contribution with a shape very similar to these theoretical curves, but sitting on top of a large, apparently diffuse background. The origin of this background is presently still undetermined, although later work has shown that it cannot be due to secondary electrons. This contribution persists when the photon energy is reduced to the point where the upper state would have to be in the gap between bands.<sup>22</sup> Under these conditions the primary electrons which we have described do not exist, and hence there are no secondaries. The emission to be expected from evanescent states at the surface also appears to be too small with respect to the emission from bulk states to explain this contribution, based on the discussion associated with Fig. 1.

The transmission factor through the surface, which is the principal subject of this work, proves to have much less effect than the polarization dependence of the matrix element which we have just discussed. In Fig. 5 we show the "average transmission factor" obtained by calculating the total photocurrent at each energy, first including the transmission factor, second with this factor set equal to 1, and then dividing the first result by the second. We find that the effect of the transmission factor is to reduce the intensity almost uniformly with energy by a factor of about 0.55. In these

calculations the transition matrix elements were not included for simplicity, but we expect that the result would not be changed by including them.

On the basis of what we observe to be happening within these calculations, we do not expect the transmission factor to have any greater effect on angular photoemission at these energies in silver. It appears that these *s* and *p* bands are free-electron-like and therefore match well with the corresponding waves in vacuum.

### V. DISCUSSION

The results obtained here explain the structure observed<sup>3</sup> in the angle dependence of the photoemission from the (111) face of silver, but not the 40% angle independent and probably incoherent background also observed. The structure obtained in our calculations arises from the same physical effects used previously by other authors to explain the shape of the experimental curves. The structure of the spectrum is dominated by the requirement that there be states at the proper energies below the Fermi level and above vacuum level with a *k* having surface components appropriate to the collection angle. The illumination angle and polarization dependence come from the angle dependence of the dipole matrix element. In particular, we find that transmission effects through the surface play practically no role in explaining the experimental data. In the future we hope to check whether these conclusions remain true when the photoemission involves excitation to *d* bands or other more localized states above the vacuum level, which might couple less strongly with plane

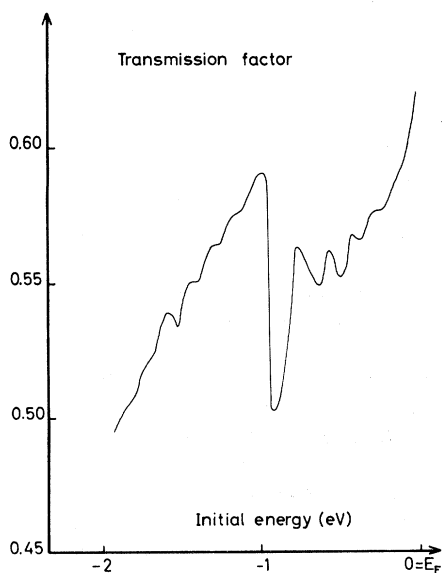


FIG. 5. "Transmission factor through the surface" (see text) as a function of energy.

waves in vacuum. Preliminary calculations have indicated that our procedures would also give a calculated photoemission from the (100) face about an order of magnitude smaller than from the (111) face, as found by Schaich,<sup>18</sup> and therefore much smaller than what is observed experimentally. This experimental emission is probably related to the diffuse component seen from the (111) face. It should be interesting to see whether including the local emission from the surface step and bulklike emission from the evanescent waves at the surface would make any contribution to this component.

The direct-transition model of photoemission limits the measured outgoing electrons to states occupying only a one-dimensional set of *k*'s in the Brillouin zone at which both the initial and final states have the selected energies. Thus the pattern of electrons coming out of the crystal should also trace out a curve in the solid angle around the crystal, i.e., a cone. Experimentally the electrons are found to come out in much broader angular distributions. This discrepancy might throw some doubt on the direct transition model if it did not give the total emission and the angular variation of the emission discussed in this paper so well. Some of the broadening can arise from the fact that the replacement of the curve of Fig. 1 by a  $\delta$  function is not exact, and the width of the peak manifests itself in a certain angular spread. Second, there is further broadening produced by phonon and diffuse surface scattering of the electrons as they come out of the crystal. Such scattering effects have been studied in the diffuse background seen in LEED experiments.<sup>41</sup> These sources of angular smearing can probably explain the spread of the angular emission discussed here which exists on top of the diffuse component. The diffuse component probably does not conserve the normal component of *k* because it is produced very near the surface.

However, simple estimates indicate that the contributions from the evanescent waves and the surface term in our equations should be quite small at these low energies so that other physical effects are probably more important. Unfortunately, the explanations suggested in the literature<sup>42,43</sup> require the treatment of surface roughness, an effect which would not be easy to include in the present method. We note that such roughness effects could also explain the apparently different results obtained by Nilsson and Eastman for the same surfaces of silver studied by Gustafsson, Nilsson, and Wallden.

### ACKNOWLEDGMENTS

The authors would like to thank J. F. Janak, A. R. Williams, and V. L. Morruzzi for the use of



their programs, and J. F. Janak in particular for help in understanding and adapting them. One of us (D.W.J.) would like to thank the Centre Europeen de Calcul Atomique et Moleculaire for a three-month stay at Orsay during which much of this work was written up.

#### APPENDIX

We show here how Eq. (A11), used in Eq. (9) of the text, can be derived. To do this we shall make extensions to a formalism developed in Ref. 29. A wave function satisfying the Bloch condition in the coordinates  $x$  and  $y$  in the surface plane can be written in the form

$$\psi(\vec{r}) = \sum_{\mathbf{K}} \psi_{\mathbf{K}}(z) e^{i(\vec{k} + \vec{K}) \cdot \vec{\rho}}, \quad \vec{\rho} = (x, y), \quad (\text{A1})$$

where the  $\vec{k}$ 's are the two-dimensional lattice vectors of the surface. It is convenient to consider matrix vectors of the form

$$\Psi = \begin{pmatrix} \{\psi_{\mathbf{K}}(z)\} \\ \{\frac{\partial \psi_{\mathbf{K}}(z)}{\partial z}\} \end{pmatrix}, \quad (\text{A2})$$

where  $\{\psi_{\mathbf{K}}(z)\}$  denotes a vector composed of all of the components of some wave function as given by Eq. (A1). Wave-function matching on a plane parallel to the surface can be done by equating  $\Psi$ 's. In terms of this vector, the flux carried by a wave function through a unit mesh parallel to the surface is proportional to

$$\Psi^\dagger X \Psi = -i \sum_{\mathbf{K}} \left( \psi_{\mathbf{K}}^* \frac{\partial \psi_{\mathbf{K}}}{\partial z} - \psi_{\mathbf{K}} \frac{\partial \psi_{\mathbf{K}}^*}{\partial z} \right),$$

where

$$X \equiv \begin{pmatrix} 0 & -i \\ +i & 0 \end{pmatrix}, \quad (\text{A3})$$

and  $\Psi^\dagger$  is the conjugate transpose of  $\Psi$ . This expression is independent of  $z$  by flux conservation, as can be readily established from the Schrödinger equation written in terms of these components. We assume here that there is no inelastic scattering, since we shall apply the result obtained only to the initial states of the photoemission process. For a Bloch wave we have

$$B_{\mathbf{k}}(\vec{r} + \vec{a}_3) = \exp(i\vec{k} \cdot \vec{a}_3) B_{\mathbf{k}}(\vec{r}), \quad (\text{A4})$$

where  $B_{\mathbf{k}} = (b_{\mathbf{k}}(z), \partial b_{\mathbf{k}}(z)/\partial z)^T$ , and  $b_{\mathbf{k}}(z)$  is a vector like  $\{\psi_{\mathbf{K}}(z)\}$  in (A2). Equation (A4) is simply a statement of the Bloch condition, which is satisfied both by the wave function and its  $z$  derivative. For

two Bloch waves with the same  $k$  we find that

$$B_{\mathbf{k}'}^\dagger(\vec{r} + \vec{a}_3) X B_{\mathbf{k}}(\vec{r} + \vec{a}_3) = \exp[i(k_z - k_z^*)a] B_{\mathbf{k}'}^\dagger(\vec{r}) X B_{\mathbf{k}}(\vec{r}). \quad (\text{A5})$$

However, the left-hand side of this equation can be shown to be independent of  $\vec{r}$  by applying flux conservation. Thus the left-hand side is equal to  $B_{\mathbf{k}'}^\dagger(\vec{r}) X B_{\mathbf{k}}(\vec{r})$  which gives

$$\{\exp[i(k_z - k_z^*)a] - 1\} B_{\mathbf{k}'}^\dagger(\vec{r}) X B_{\mathbf{k}}(\vec{r}) = 0, \quad (\text{A6})$$

showing directly that the cross terms between Bloch waves do not carry current, a result which is usually assumed from the fact that packets made up of the two waves will physically separate with time. The consequences for evanescent waves are even more interesting, but cannot be discussed here.

We shall now make the change of normalization

$$\tilde{B}_{\mathbf{k}} = |B_{\mathbf{k}}^\dagger X B_{\mathbf{k}}|^{-1/2} B_{\mathbf{k}}, \quad (\text{A7})$$

so that the Bloch waves moving into the crystal form an orthonormal system using the flux expression (A3) as an inner product. A typical photoemission initial state has the form

$$\Psi_v = \tilde{B}_v^- + \sum_j \tilde{\beta}_{vj} \tilde{B}_j^+, \quad (\text{A8})$$

where  $\tilde{B}_v^-$  is a propagating Bloch wave moving toward the surface and the  $\tilde{B}_j^+$ 's are propagating Bloch wave moving back from the surfaces and evanescent Bloch waves decaying away from the surface.

Since no linear combination of these initial states can carry flux across the surface plane into vacuum we have

$$0 = \Psi_v^\dagger X \Psi_v = \tilde{B}_v^{-\dagger} X \tilde{B}_v^+ + \sum_{j,l} \tilde{\beta}_{vj}^* \tilde{\beta}_{vl} \tilde{B}_j^{+\dagger} X \tilde{B}_l^+,$$

where we have dropped the cross terms between the (-) and (+) Bloch waves which are zero because of Eq. (A6). Using this same equation we may drop all evanescent waves and all cross terms between the (+) propagating waves because they make no contribution. In this way we obtain

$$0 = -\delta_{vl} + \sum_j \tilde{\beta}_{vj}^* \tilde{\beta}_{lj}, \quad (\text{A9})$$

in which only the  $\beta$ 's corresponding to propagating waves are included. From Eq. (A9) we conclude that these  $\beta$ 's form a unitary matrix. This implies that we also have

$$\sum_v \tilde{\beta}_{vj}^* \tilde{\beta}_{vl} = \delta_{jl}. \quad (\text{A10})$$

If we now revert to Bloch waves which are normalized to integrate to 1 over a unit cell (and the incident wave is also so normalized) and choose  $j=l$

this becomes

$$\sum_{\nu} |\beta_{\nu j}|^2 \frac{1}{v_{\nu}} = \frac{1}{v_j}, \quad (\text{A11})$$

which is the result required when we consider a

Bloch wave moving into the crystal in Eq. (9). For a Bloch wave moving toward the surface the required result is trivial. We note from this discussion that the unit flux normalization is really the appropriate one for this problem.

\*Present address: Laboratoire de Physique des Solides, Université Paris-Sud, Centre D'Orsay, 91405-Orsay, France.

<sup>1</sup>G. W. Gobeli, F. G. Allen, and E. O. Kane, *Phys. Rev. Lett.* **12**, 94 (1964).

<sup>2</sup>U. Gerhardt and E. Dietz, *Phys. Rev. Lett.* **26**, 1477 (1971).

<sup>3</sup>T. Gustafsson, P. O. Nilsson, and L. Wallden, *Phys. Lett. A* **37**, 121 (1971).

<sup>4</sup>R. Y. Koyama and L. R. Hughey, *Phys. Rev. Lett.* **29**, 1518 (1972).

<sup>5</sup>F. Wooten, T. Huen, and H. V. Winsor, *Phys. Lett. A* **36**, 351 (1971).

<sup>6</sup>L. Wallden and T. Gustafsson, *Phys. Scripta* **6**, 73 (1972).

<sup>7</sup>B. Feurbacher and B. Fitton, *Phys. Rev. Lett.* **30**, 923 (1973).

<sup>8</sup>P. O. Nilsson and D. E. Eastman, *Phys. Scripta* **8**, 113 (1973).

<sup>9</sup>N. V. Smith and M. M. Traum, *Phys. Rev. Lett.* **31**, 1247 (1973).

<sup>10</sup>M. M. Traum, N. V. Smith, and F. J. Di Salvo, *Phys. Rev. Lett.* **32**, 1241 (1974).

<sup>11</sup>N. V. Smith, M. M. Traum, and F. J. Di Salvo, *Solid State Commun.* **15**, 211 (1974).

<sup>12</sup>R. R. Turtle and T. A. Callcott, *Phys. Rev. Lett.* **34**, 86 (1974).

<sup>13</sup>W. F. Egelhoff and D. L. Perry, *Phys. Rev. Lett.* **34**, 93 (1975).

<sup>14</sup>E. O. Kane, *Phys. Rev. Lett.* **12**, 97 (1964).

<sup>15</sup>G. D. Mahan, *Phys. Rev. Lett.* **24**, 1068 (1970); also Ref. 20.

<sup>16</sup>B. J. Wacławski and E. W. Plummer, *Phys. Rev. Lett.* **29**, 783 (1972).

<sup>17</sup>B. Feurbacher and B. Fitton, *Phys. Rev. Lett.* **29**, 786 (1972).

<sup>18</sup>W. L. Schaich, Fourth International Conference on Vacuum-ultraviolet Radiation Physics, Hamburg, Germany, July 22-26, 1974 (unpublished).

<sup>19</sup>C. N. Berglund and W. E. Spicer, *Phys. Rev.* **136**, A1030 (1964).

<sup>20</sup>I. Adawi, *Phys. Rev.* **134**, A788 (1964).

<sup>21</sup>G. D. Mahan, *Phys. Rev. B* **2**, 4334 (1970).

<sup>22</sup>P. O. Nilsson (private communication); background exists without primaries.

<sup>23</sup>Reference 20, Eq. (2.13b).

<sup>24</sup>Other procedures for obtaining the normalization and density of states give the same results for the product, which is a bulk quantity, independent of the choice of states.

<sup>25</sup>P. J. Feibelman and D. E. Eastman, *Phys. Rev. B* **10**, 4932 (1974).

<sup>26</sup>D. W. Jepsen, P. M. Marcus, and F. Jona, *Phys. Rev. B* **5**, 3933 (1972).

<sup>27</sup>J. A. Strozier, Jr., D. W. Jepsen, and F. Jona, in *Surface Physics of Crystalline Materials*, edited by J. M. Blakely (Academic, New York, 1975).

<sup>28</sup>J. B. Pendry, *Low Energy Electron Diffraction* (Academic, New York, 1974).

<sup>29</sup>D. W. Jepsen and P. M. Marcus, *Computational Methods in Band Theory* (Plenum, New York, 1971), p. 416.

<sup>30</sup>See Ref. 38 below and the associated discussion in the text.

<sup>31</sup>K. Mitchell, *Proc. R. Soc. A* **146**, 422 (1934).

<sup>32</sup>R. E. B. Makinson, *Proc. R. Soc. A* **162**, 367 (1937).

<sup>33</sup>A. R. Williams, J. F. Janak, and V. L. Maruzzi, *Phys. Rev. Lett.* **28**, 672 (1972).

<sup>34</sup>Reference 26, Eq. (10); also Ref. 29, Eq. (19).

<sup>35</sup>See Ref. 27, p. 18.

<sup>36</sup>E. C. Snow, *Phys. Rev.* **172**, 708 (1968).

<sup>37</sup>L. R. Canfield and G. Haas, *J. Opt. Soc. Am.* **55**, 61 (1965); G. B. Irani, T. Huen, and F. Wooten, *ibid.* **61**, 128 (1971).

<sup>38</sup>H. Kanter, *Phys. Rev. B* **1**, 522 (1970).

<sup>39</sup>E. O. Kane, *Phys. Rev.* **159**, 624 (1967).

<sup>40</sup>D. Spanjaard, D. W. Jepsen, P. M. Marcus (unpublished).

<sup>41</sup>R. F. Barnes, M. G. Lagally, and M. B. Webb, *Phys. Rev.* **171**, 627 (1968).

<sup>42</sup>J. G. Endriz and W. E. Spicer, *Phys. Rev. B* **4**, 4159 (1971).

<sup>43</sup>D. Grant and P. R. Cutler, *Phys. Rev. Lett.* **31**, 1171 (1973).